Table 1
Characteristics of participants according to FABP2 Ala54Thr (G/A) genotype.

Genotype	GG	GA	AA	p
N	584 (40.9%)	672 (47.1%)	172 (12.0%)	
Age	62.8 ± 0.4	63.4 ± 0.4	63.0 ± 0.7	NS
AHT (dB)	20.1 ± 0.5	20.2 ± 0.5	21.8 ± 1.0	NS
Serum triglyceride (mg/dl)	120.9 ± 3.0	115.6 ± 2.8	114.9 ± 5.6	NS
Sex (male %)	48.6	53.9	54.7	NS
Hearing impairment (%)	25.0	25.0	34.3	0.0336

AHT: average hearing threshold level for frequencies 500,1000,2000, and 4000 Hz for the better ear. Mean ± standard error. NS: not significant. Hearing impairment: AHT > 25 dB. p-Value tested by the analysis of variance or χ^2 test.

Under the recessive model of inheritance, the risk for hearing impairment increased significantly in mutant homozygotes. The significant association of the FABP2 Ala54Thr polymorphism with hearing impairment was independent of the presence of diabetes or obesity.

4. Discussion

In a population-based sample of middle-aged and elderly Japanese, the Thr54 variant of FABP2 gene had a significant adverse effect on hearing. The FABP2 is found exclusively in the epithelium of the small intestine, therefore, the etiological role of the gene polymorphism on hearing impairment is likely to be indirect. Since the effect on hearing may be due to various confounders associated with Thr54, possible risk-modifying factors, including diabetes and obesity, should be taken into account in analyses. After adjustment for confounders, a significant effect of the Thr54 variant on hearing was observed in the additive and recessive models and the effect was independent of both diabetes and obesity.

Several studies have shown the association between the Ala54Thr polymorphism with variations in fatty acid absorption and insulin resistance. The Ala54Thr variant FABP2 results in increased fatty acid uptake from the intestinal lumen, since variant (Thr54-containing) FABP2 binds fatty acid with twofold greater affinity than wild-type Ala54-containing protein [7]. It has been reported that carriers of the Thr54 variant had lower peripheral insulin sensitivity and an increased concentration of free fatty acids after the intake of a diet rich in saturated fats [8]. Regarding an association between the Thr54 allele and dyslipidemia, the findings from previously reported studies have not always been consistent. The present study did not show an association between the Ala54Thr polymorphism and fasting triglyceride concentration. Postprandial lipemia in Thr54 carriers had been dependent on the type of fat ingested when diet–gene interactions of FABP2 Ala54Thr were tested using 3 different diets [9]. Gene–environment interactions or variation in the FABP2 promoter region may also have a role in accounting for some of the observed phenotypic differences in lipid metabolism between carriers of the Thr54 polymorphism across populations [10,11].

One speculative hypothesis about the influence of FABP2 gene polymorphism in the aged population is caloric restriction theory. Since McCay et al. first reported that

Table 2
Odds ratios of hearing impairment and comparison of hearing level among FABP2 genotypes.

Mode of inheritance			GG (A = 0)	GA (A = 1)	AA (A = 2)	p
Additive genetic model[a]	Number		584	672	172	
	Per-allele odds ratios	Model 1	1	1.262 (1.012–1.574)/A allele		0.0386
		Model 2	1	1.259 (1.009–1.571)/A allele		0.0410
Mode of inheritance			GG	GA/AA		p
Dominant genetic model	Number		584	844		
	Odds ratios	Model 1	1	1.085 (0.802–1.468)		NS
		Model 2	1	1.081 (0.799–1.463)		NS
Mode of inheritance			GG/GA	AA		p
Recessive genetic model	Number		1256	172		
	Odds ratios	Model 1	1	2.096 (1.366–3.216)		0.0007
		Model 2	1	2.097 (1.365–3.221)		0.0007

Moderator variable – Model 1: age, sex, history of ear disease, and history of occupational noise exposure. Model 2: history of heart disease, history of hypertension, diabetes, and BMI, in addition to those in model 1. Parenthetical reference shows 95% confidence interval. *Abbreviations*: BMI: body mass index. NS: not significant.

[a] The additive genetic model assumes that there is a linear gradient in risk between the GG, GA and AA genotypes (GG genotype base). This is equivalent to a comparison of the A allele versus the G allele. The per-allele odds ratio for hearing impairment risk is shown under the additive genetic model.

Please cite this article in press as: Uchida Y, et al. The Ala54Thr polymorphism in the fatty acid-binding protein 2 (FABP2) gene is associated with hearing impairment: A preliminary report. Auris Nasus Larynx (2010), doi:10.1016/j.anl.2010.01.006

restricting the food intake of laboratory rats dramatically increased their life span [12], caloric restriction has been touted as the most effective way to extend the lifespan of mammals [13]. This increase in longevity is coupled to profound beneficial effects on age-related pathology [14]. Mechanisms postulated to be responsible for the effects of caloric restriction include altered gene expression, reduced oxidative stress, decreased metabolism, and increased DNA repair capacity [15]. Previous studies demonstrated that caloric restriction had significant effects to retard age-related hearing loss. Caloric restriction has been shown to suppress apoptotic cell death in the mouse cochlea and to lower quantity of mitochondrial DNA deletions in the cochlea [16,17]. Taking these findings together, the present results might be potentially explained by invoking the function of the Ala54Thr variant FABP2 in energy metabolism.

5. Conclusion

A significant association between the Ala54Thr polymorphism of FABP2 and hearing was observed in a population-based sample of middle-aged and elderly Japanese. Although carriers of the Thr54 variant have been reported to be associated with lower peripheral insulin sensitivity and an increased concentration of free fatty acids, the significant adverse effect of the Thr54 variant on hearing was independent of both diabetes and obesity in the present analyses. The results might support caloric restriction theory indirectly, but additional researches are desired.

Conflicts of interest

There are no conflicts of interest.

Acknowledgments

We thank all of the participants, and also the health professionals and the researchers from the department of Epidemiology, National Center for Geriatrics and Gerontology, who were involved in the data collection and analyses.

This study was partially supported by a Grant-in-Aid for Comprehensive Research on Aging and Health, from the Ministry of Health, Labour and Welfare of Japan (H17-choju-ippan-033).

References

[1] Sweetser DA, Birkenmeier EH, Klisak IJ, Zollman S, Sparkes RS, Mohandas T, et al. The human and rodent intestinal fatty acid binding protein genes. A comparative analysis of their structure, expression, and linkage relationships. J Biol Chem 1987;262:16060–71.

[2] Baier LJ, Bogardus C, Sacchettini JC. A polymorphism in the human intestinal fatty acid binding proteins alters fatty acid transport across Caco-2 cells. J Biol Chem 1996;271:10892–6.

[3] Bainbridge KE, Hoffman HJ, Cowie CC. Diabetes and hearing impairment in the United States: audiometric evidence from the National Health and Nutrition Examination Survey, 1999 to 2004. Ann Intern Med 2008;149:1–10.

[4] Fransen E, Topsakal V, Hendrickx JJ, Van Laer L, Huyghe JR, Van Eyken E, et al. Occupational noise, smoking, and a high body mass index are risk factors for age-related hearing impairment and moderate alcohol consumption is protective: a European population-based multicenter study. J Assoc Res Otolaryngol 2008;9:264–76.

[5] Shimokata H, Ando F, Niino N. A new comprehensive study on aging—the National Institute for Longevity Sciences, Longitudinal Study of Aging (NILS-LSA). J Epidemiol 2000;10:S1–9.

[6] Uchida Y, Sugiura S, Nakashima T, Ando F, Shimokata H. Endothelin-1 gene polymorphism and hearing impairment in elderly Japanese. Laryngoscope 2009;119:938–43.

[7] Baier LJ, Sacchettini JC, Knowler WC, Eads J, Paolisso G, Tataranni PA, et al. An amino acid substitution in the human intestinal fatty acid binding protein is associated with increased fatty acid binding, increased fat oxidation, and insulin resistance. J Clin Invest 1995;95:1281–7.

[8] Marín C, Pérez-Jiménez F, Gómez P, Delgado J, Paniagua JA, Lozano A, et al. The Ala54Thr polymorphism of the fatty acid-binding protein 2 gene is associated with a change in insulin sensitivity after a change in the type of dietary fat. Am J Clin Nutr 2005;82:196–200.

[9] Dworatzek PD, Hegele RA, Wolever TM. Postprandial lipemia in subjects with the threonine 54 variant of the fatty acid-binding protein 2 gene is dependent on the type of fat ingested. Am J Clin Nutr 2004;79:1110–7.

[10] Paglialunga S, Cianflone K. Regulation of postprandial lipemia: an update on current trends. Appl Physiol Nutr Metab 2007;32:61–75.

[11] Formanack ML, Baier LJ. Variation in the FABP2 promoter affects gene expression: implications for prior association studies. Diabetologia 2004;47:349–51.

[12] McCay CM, Crowell MF, Maynard LA. The effect of retarded growth upon length of lifespan and upon ultimate body size. J Nutr 1935;10:63–79.

[13] Masoro EJ. Caloric restriction and aging: an update. Exp Gerontol 2000;35:299–305.

[14] Mair W, Dillin A. Aging and survival: the genetics of life span extension by dietary restriction. Annu Rev Biochem 2008;77:727–54.

[15] Lee CK, Klopp RG, Weindruch R, Prolla TA. Gene expression profile of aging and its retardation by caloric restriction. Science 1999;285:1390–3.

[16] Someya S, Yamasoba T, Weindruch R, Prolla TA, Tanokura M. Caloric restriction suppresses apoptotic cell death in the mammalian cochlea and leads to prevention of presbycusis. Neurobiol Aging 2007;28:1613–22.

[17] Yamasoba T, Someya S, Yamada C, Weindruch R, Prolla TA, Tanokura M. Role of mitochondrial dysfunction and mitochondrial DNA mutations in age-related hearing loss. Hear Res 2007;226:185–93.

Please cite this article in press as: Uchida Y, et al. The Ala54Thr polymorphism in the fatty acid-binding protein 2 (FABP2) gene is associated with hearing impairment: A preliminary report. Auris Nasus Larynx (2010), doi:10.1016/j.anl.2010.01.006

Acta Oto-Laryngologica, 2010; Early Online, 1–7

informa
healthcare

ORIGINAL ARTICLE

Relationship between endolymphatic hydrops and vestibular-evoked myogenic potential

NAOMI KATAYAMA[1,2], MASAKO YAMAMOTO[2], MASAAKI TERANISHI[2], SHINJI NAGANAWA[3], SEIICHI NAKATA[2], MICHIHIKO SONE[2] & TSUTOMU NAKASHIMA[2]

[1]*Department of Nutrition and Food Science, Nagoya Women's University,* [2]*Department of Otorhinolaryngology and* [3]*Department of Radiology, Nagoya University, Graduate School of Medicine, Nagoya, Japan*

Abstract

Conclusion: Vestibular-evoked myogenic potential (VEMP) can be used to examine endolymphatic hydrops, especially in the vestibule. *Objective:* To investigate the relationship between the degree of endolymphatic hydrops revealed by magnetic resonance imaging (MRI) and VEMP. *Methods:* Gadolinium diluted with saline was injected intratympanically in 49 ears (40 patients). One day after the injection, the endolymphatic space in the vestibule and the cochlea was visualized by 3 Tesla MRI. A VEMP test was done, and VEMP was judged as absent when the VEMP was within the noise level. *Results:* VEMP was present in 21 ears and absent in 28 ears. Endolymphatic hydrops was significantly associated with the disappearance of VEMP. Endolymphatic hydrops in the vestibule had a stronger effect than endolymphatic hydrops in the cochlea. Five patients with extremely large vestibular hydrops showed no response of VEMP.

Keywords: *Ménière's disease, MRI, endolymphatic space*

Introduction

Vestibular-evoked myogenic potential (VEMP) is now widely used to examine otolith function, especially saccular function. VEMP may be reduced or abolished in patients with endolymphatic hydrops in the vestibule [1–3]. However, Young *et al.* [3] reported that augmentation of VEMP may be recognized in cases with extremely large endolymphatic hydrops in which the endolymphatic space contacts the stapes footplate.

Recently, we visualized endolymphatic hydrops after intratympanic gadolinium (Gd) injection using 3 Tesla magnetic resonance imaging (MRI) [4]. We investigated the relationship between endolymphatic hydrops and VEMP.

Material and methods

Patients

The subjects included 49 ears sampled in 40 patients. There were 19 patients with definite Ménière's disease defined by the criteria of the 1995 American Academy of Otolaryngology-Head and Neck Surgery (AAO-HNS) guidelines [5] (group A). Four patients had fluctuating hearing loss with disequilibrium but without definitive episodes of vertigo attacks (group B). Two patients had episodic vertigo of the Ménière type without documented hearing loss (group C). According to the criteria of the 1995 AAO-HNS, groups B and C are defined as possible Ménière's disease. There were three patients with fluctuating

Correspondence: Tsutomu Nakashima MD, Department of Otorhinolaryngology, Nagoya University, Graduate School of Medicine, 65, Tsurumai-cho, Showa-ku, Nagoya, 466-8550, Japan. Tel: +85 52 744 2323. Fax: +85 52 744 2325. E-mail: tsutomun@med.nagoya-u.ac.jp

(Received 14 October 2009; accepted 13 December 2009)

ISSN 0001-6489 print/ISSN 1651-2251 online
DOI: 10.3109/00016480903573187

hearing loss without disequilibrium or vertigo (group D). This atypical Ménière's disease involving fluctuating hearing loss without vertigo was defined as cochlear Ménière's disease by the subcommittee on equilibrium and its measurement of the American Academy of Ophthalmology and Otolaryngology (AAOO) in 1972 [6], but was not included in Ménière's disease defined by the 1995 AAO-HNS criteria [5].

Eight patients were diagnosed as having delayed endolymphatic hydrops according to the previous reports [7,8]. Of eight patients, there were two patients with ipsilateral type. Six patients had contralateral or bilateral type. Four patients had sudden sensorineural hearing loss defined by the criteria described by the Sudden Deafness Research Committee of the Ministry of Health and Welfare, Japan [9]. Three patients with bilateral hearing fluctuation, one patient in group C and five patients with contralateral or bilateral delayed endolymphatic hydrops underwent the examination bilaterally. Table I shows the details of the patients with hearing level examined by an audiometer (AA-79S, Rion Co. Ltd, Tokyo, Japan).

The protocol was approved by the Ethics Review Committee of Nagoya University School of Medicine (approval no. 369, 1–4). All patients gave informed consent for participation. Their written informed consent was attached to the electronic medical record with permission of the patient, in accordance with the Ethics Review Committee.

Intratympanic gadolinium injection and MRI

The detailed methods for intratympanic gadolinium (Gd) injection and MRI have been reported previously [4,10,11]. Briefly, Gd contrast material (Omniscan® or Magnevist®) was diluted eightfold or 16-fold with saline. The diluted Gd was injected through the tympanic membrane using a 23 gauge needle and a 1 ml syringe after the patient was placed in the supine position with his/her head turned approximately 30° away from the sagittal line towards the opposite ear. The amount of diluted Gd injected was 0.4–0.5 ml. After the injection, the patient remained in the supine position for 60 min with his/her head turned approximately 60° away from the sagittal line toward the opposite ear.

MRI scans were performed with a 3 T unit (Trio, Siemens, Erlangen, Germany). Three-dimensional fluid attenuated inversion recovery (3D-FLAIR) and three-dimensional inversion recovery (3D-real IR) MRI were used for evaluation of the endolymphatic space [11].

Image evaluation

The degrees of endolymphatic hydrops in the vestibule and cochlea were classified into three groups: 'none,' 'mild,' and 'significant,' according to criteria described previously [12]. A radiologist who did not know the results of VEMP evaluated the degree of hydrops in the vestibule and in the cochlea.

In the vestibule, the grading was determined by the ratio of the area of the endolymphatic space to the vestibular fluid space (sum of the endolymphatic and perilymphatic spaces). Patients with no hydrops had a ratio of one-third or less, those with mild hydrops had between one-third and half, and those with significant hydrops had a ratio of more than half. In the cochlea, patients classified as having no hydrops showed no displacement of the Reissner's membrane; those with mild hydrops showed displacement of the Reissner's membrane, but the area of the endolymphatic space

Table I. Number of ears examined with Ménière's disease, delayed endolymphatic hydrops, and sudden sensorineural hearing loss.

Group	No. of patients	Average age (years)	No. of males	No. of females	No. of ears examined	Average hearing level (dB)
Ménière's disease group A	19	53.7	10	9	21	39.4
Ménière's disease group B	4	62.8	2	2	5	33.6
Ménière's disease group C	2	52	1	1	3	12.2
Ménière's disease group D	3	53.7	1	2	3	30.3
Ipsilateral DEH	2	30	1	1	2	87
Contralateral or bilateral DEH	6	45.8	4	2	11	74.2
Sudden sensorineural hearing loss	4	50.5	2	2	4	69.3

Ménière's disease group A, definite Ménière's disease; group B, possible Ménière's disease that had fluctuating hearing loss with disequilibrium but without definitive episodes of vertigo attacks; group C, possible Ménière's disease that had episodic vertigo of the Ménière type without documented hearing loss; group D, 'cochlear Ménière's disease' involving fluctuating hearing loss without disequilibrium or vertigo; DEH, delayed endolymphatic hydrops. Average hearing level is the average of three frequencies of 500 Hz, 1 kHz, and 2 kHz.

did not exceed the area of the scala vestibule. In those with significant hydrops, the area of the endolymphatic space exceeded the area of the scala vestibuli [12].

VEMP

Surface myogenic potentials in the sternocleidomastoid muscle were added 150 times with a reference electrode over the sternum while clicks (105 dB) were presented to the ipsilateral ear and white noise (75 dB) was presented to the contralateral ear (Synax 2100, NEC Medical Systems, Tokyo, Japan). The ground electrode was on the forehead. The stimulation rate of the clicks was 5 Hz, and the electromyogenic signal was amplified through a bandpass filter (20–2000 Hz). The patient was instructed to turn his/her head toward the contralateral side in the sitting position to activate the sternomastoid muscle. When VEMP was recognized above the noise level, it was judged as VEMP present. Decreased VEMP was judged as VEMP present if the waveform was recognized [13]. When VEMP was within noise level, it was judged as VEMP absent.

Statistical analysis

Data were analyzed using STATA 8. χ^2 test, Mann–Whitney test, and multivariate analysis were done. Statistical significance was judged as present when the p value was < 0.05.

Results

Thirteen ears had no hydrops, 10 ears had mild hydrops, and 26 ears had significant hydrops in the vestibule. In the cochlea, 13 ears had no hydrops, 16 ears had mild hydrops, and 20 ears had significant hydrops. Examples of no, mild, and significant hydrops in the vestibule are shown in Figs 1, 2, and 3, respectively. Figure 4 shows an example of extremely large endolymphatic hydrops among patients with significant hydrops in the vestibule. These figures are suitable sections for evaluation of hydrops in the vestibule. Figure 5 shows an example of suitable section for evaluation of hydrops in the cochlea.

Table II summarizes the results of MRI and VEMP in each group. In patients with definite Ménière's disease, hydrops was observed in both the cochlea and the vestibule except for one patient. In patients who had episodic vertigo of the Ménière type without documented hearing loss (group C) and patients with sudden sensorineural hearing loss, no hydrops was observed in MRI.

Figure 1. MRI of the left inner ear after intratympanic administration in a patient who had episodic vertigo of the Ménière type without documented hearing loss. No endolymphatic hydrops was observed.

VEMP was present in 21 ears and was absent in 28 ears. Examples of present and absent VEMP are shown in Figs 6 and 7, respectively. In patients who had episodic vertigo of the Ménière type without documented hearing loss (group C) and patients with sudden sensorineural hearing loss, VEMP was present.

Table III shows the relationship between VEMP and vestibular hydrops revealed by the MRI. In 13 ears with no vestibular hydrops on the MRI, VEMP was present in 10 ears and was absent in 3 ears. In 36 ears with vestibular hydrops on MRI, VEMP was present in 11 ears and was absent in 25 ears. In patients with vestibular hydrops on the MRI, the percentage of absent VEMP was significantly high. χ^2 tests revealed significant differences (2×2 contingency table, $p < 0.01$; 3×2 contingency table, $p < 0.05$). All five patients who had extremely large vestibular hydrops showed no response of VEMP.

Table IV shows the relationship between VEMP and the cochlear hydrops revealed by the MRI. In 13 ears with no cochlear hydrops on the MRI, VEMP was present in 9 ears and was absent in 4 ears. In 36 ears with cochlear hydrops on MRI, VEMP was present 12 ears and was absent in 24 ears. In patients with cochlear hydrops on the MRI, the percentage of absent VEMP was high (2×2 contingency table, χ^2 test, $p < 0.05$).

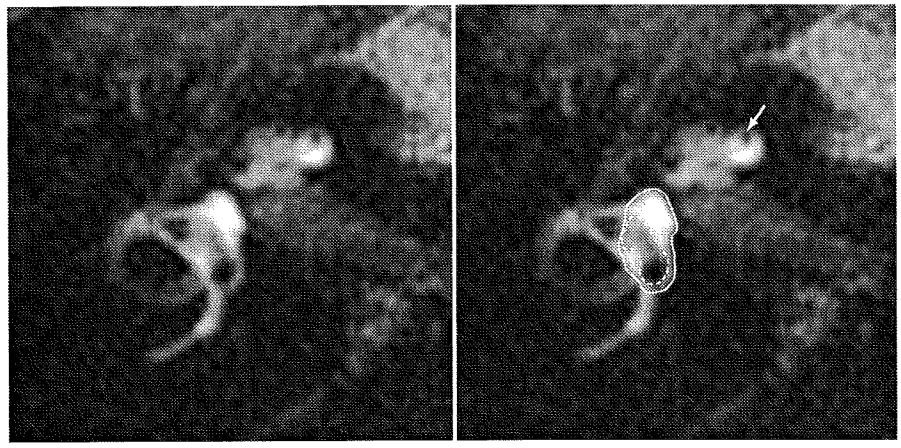

Figure 2. MRI of the right inner ear after intratympanic Gd administration in a patient with definite Ménière's disease. Left side, original MRI. Right side, line drawings on the original MRI. Dotted line shows the endolymphatic space in the vestibule (solid line). The area ratio of the endolymphatic space to the vestibule area was 38% (mild hydrops in the vestibule). White arrow indicates endolymphatic hydrops in the basal turn of the cochlea.

We performed multivariate analysis to investigate how the endolymphatic hydrops affects the VEMP results. Regression analysis was as follows.

$X = -0.164\ X_1 - 0.078\ X_2 + 0.730$

$X = 1$, VEMP present; $X = 0$, VEMP absent. X_1, degree of hydrops in the vestibule (none = 0, mild = 1, significant = 2); X_2, degree of hydrops in the cochlea (none = 0, mild = 1, significant = 2). This equation had statistical significance ($p < 0.05$).

When the coefficients X_1 and X_2 are compared, the endolymphatic hydrops in the vestibule had a stronger effect on the disappearance of VEMP than did endolymphatic hydrops in the cochlea. X was obtained in each ear. Of 21ears with VEMP response, X was ≥ 0.49 in 13 ears (62%). Of 28 ears without VEMP response, X was < 0.49 in 20 ears (71%).

The average age in the VEMP absent and present groups was 49.9 ± 12.5 years and 46.7 ± 14.9 years, respectively. Average hearing level of three frequencies of 500 Hz, 1 kHz, and 2 kHz were 45.0 ± 23.3 dB and 47.2 ± 37.3 dB in VEMP absent and present groups, respectively. Thus, hearing level was not associated with the VEMP results.

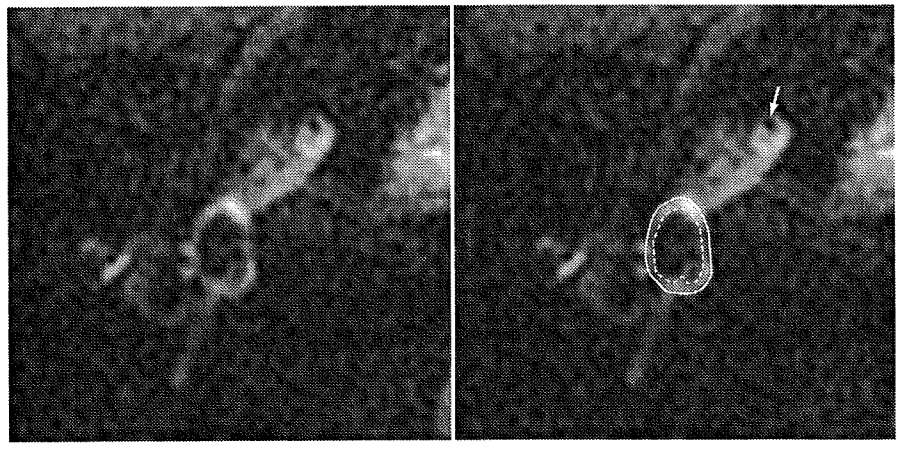

Figure 3. MRI of the right inner ear after intratympanic Gd administration in a patient with delayed endolymphatic hydrops. Left side, original MRI. Right side, line drawings on the original MRI. Dotted line shows the endolymphatic space in the vestibule (solid line). The area ratio of the endolymphatic space to the vestibule area was 62% (significant hydrops in the vestibule). White arrow indicates endolymphatic hydrops in the basal turn of the cochlea.

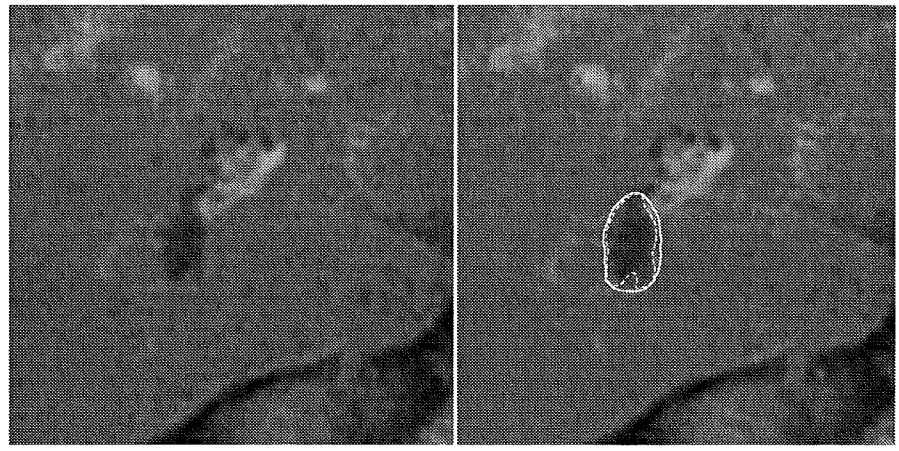

Figure 4. MRI of the right inner ear after intratympanic Gd administration in a patient with definite Ménière's disease. Left side, original MRI. Right side, line drawings on the original MRI. Dotted line shows extremely large endolymphatic hydrops in the vestibule. The area ratio of the endolymphatic space to the vestibule area shown with the solid line was 84% (extremely large endolymphatic hydrops in the vestibule).

Presence or absence of vertigo had no significant relationship with VEMP. The period from the onset of clinical symptoms to the examination also had no effect on the result of VEMP. The period from the onset of clinical symptoms to the examination ranged from 1 to 242 months in the VEMP absent group and from 1 to 354 months in the VEMP present group. No difference in the period was observed between the two groups (Mann–Whitney test).

Discussion

Several authors have described the relationship between endolymphatic hydrops and the disappearance of VEMP from the results of functional tests [1,2]. Our MRI study revealed a significant relationship between endolymphatic hydrops and VEMP. Endolymphatic hydrops in the vestibule had a stronger effect than endolymphatic hydrops in the cochlea. Because VEMP is a saccular function, endolymphatic hydrops in the vestibule may be strongly associated with the VEMP.

Young *et al.* [3] reported that VEMP may be increased when endolymphatic hydrops in the vestibule is extremely large as endolymphatic space contacts with the stapes footplate. However, in our study, VEMP was absent in all five ears in which the vestibule was occupied by extremely large endolymphatic hydrops in MRI. It seemed that the augumentation of VEMP that was

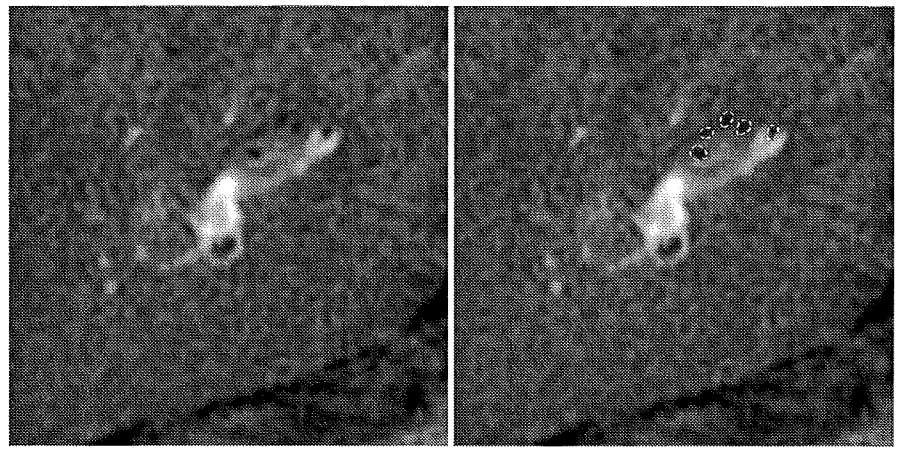

Figure 5. An example of endolymphatic hydrops in the right cochlea. Left side, original MRI. Right side, line drawings on the original MRI. Endolymphatic hydrops is shown with dotted lines in the upper and lower turns of the cochlea.

Table II. Number of ears that showed no, mild, or significant hydrops in the vestibule and the cochlea in Ménière's disease, delayed endolymphatic hydrops, and sudden sensorineural hearing loss.

				MRI hydrops					
		VEMP		Vestibule			Cochlea		
Group	No. of ears	Present	Absent	None	Mild	Significant	None	Mild	Significant
Ménière's disease group A	21	4	17	1	6	14	0	7	14
Ménière's disease group B	5	2	3	1	0	4	1	2	2
Ménière's disease group C	3	3	0	3	0	0	3	0	0
Ménière's disease group D	3	0	3	0	2	1	1	1	1
Ipsilateral DEH	2	1	1	1	1	0	1	1	0
Contralateral or bilateral DEH	11	7	4	3	1	7	3	5	3
Sudden sensorineural hearing loss	4	4	0	4	0	0	4	0	0

See footnotes to Table I for explanation of groups.

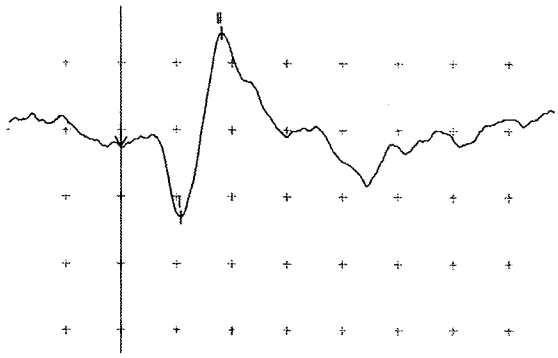

Figure 6. An example of VEMP response.

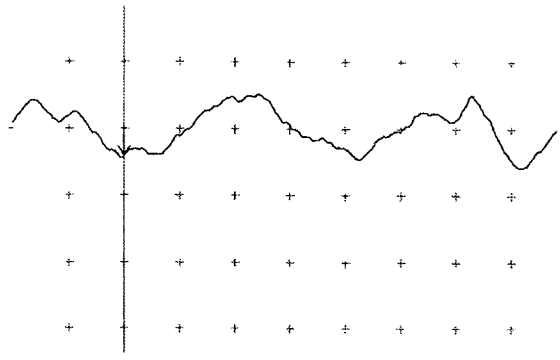

Figure 7. An example of absent VEMP.

described by Young *et al.* [3] in patients with extremely large endolymphatic hydrops was rare.

de Waele *et al.* [14] reported that VEMP was absent on the affected side in 54% of the patients with Ménière's disease. This absence correlated with the degree of low frequency hearing loss but not with

Table III. Relationship between VEMP and vestibular hydrops revealed by MRI.

	VEMP	
Vestibular hydrops	Present (no. of ears)	Absent (no. of ears)
None	10	3
Mild	3	7
Significant	8	18

Table IV. Relationship between VEMP and cochlear hydrops revealed by MRI.

	VEMP	
Cochlear hydrops	Present (no. of ears)	Absent (no. of ears)
None	9	4
Mild	6	10
Significant	6	14

canal paresis. On the contrary, Ushio *et al.* [15] described that absence or presence of VEMP was independent of the results of pure tone audiometry and auditory brain stem responses. We observed that the disappearance of VEMP was not associated with the hearing level.

Our MRI study also revealed that there were cases in which VEMP was present even if endolymphatic hydrops was significant in the vestibule. This situation is similar to that of electrocochleography in patients with Ménière's disease. The average summating potential to action potential (SP/AP) ratio was high in patients with significant endolymphatic hydrops in the cochlea. But the SP/AP ratio was not enlarged in some patients with a relatively short period from the onset of clinical

symptoms to the electrocochleography examination in spite of significant endolymphatic hydrops in the cochlea [16]. This may imply that elevation of the SP/AP ratio is related not only to the degree of endolymphatic hydrops but also to the persistence of hydrops. In the present study, the period from the onset of clinical symptoms to the examination also had no effect on the result of VEMP. Because our study included various types of inner ear diseases, the relationship between the VEMP result and the duration of the disease should be studied further.

We can now image endolymphatic hydrops using advanced MRI technology in living patients. At present, however, we cannot find differences in the MRI between definite Ménière's disease and 'cochlear Ménière's disease' [17]. On the contrary, endolymphatic hydrops was not recognized in patients who had episodic vertigo of the Ménière type without documented hearing loss in the present study. Reduction of endolymphatic hydrops could be observed when the MRI was carried out twice or more with alleviation of the symptoms in patients with Ménière's disease [18,19]. MRI carried out before and after the vertigo attacks will provide a new aspect for understanding the mechanism of the vertigo attacks. It has been reported that VEMP recovers to normal in some patients with Ménière's disease after administration of furosemide [20]. A dynamic relationship between endolymphatic hydrops and VEMP may be a future topic.

Acknowledgment

This study was supported by research grants from the Ministry of Health, Labour and Welfare and the Ministry of Education, Culture, Sports, Science & Technology in Japan.

Declaration of interest: The authors report no conflicts of interest. The authors alone are responsible for the content and writing of the paper.

References

[1] Magliulo G, Cuiuli G, Gagliardi M, Ciniglio-Appiani G, D'Amico R. Vestibular evoked myogenic potentials and glycerol testing. Laryngoscope 2004;114:338–43.

[2] Lin MY, Timmer FC, Oriel BS, Zhou G, Guinan JJ, Kujawa SG, et al. Vestibular evoked myogenic potentials (VEMP) can detect asymptomatic saccular hydrops. Laryngoscope 2006;116:987–92.

[3] Young YH, Wu CC, Wu CH. Augmentation of vestibular evoked myogenic potentials: an indication for distended saccular hydrops. Laryngoscope 2002;112:509–12.

[4] Nakashima T, Naganawa S, Sugiura M, Teranishi M, Sone M, Hayashi H, et al. Visualization of endolymphatic hydrops in patients with Meniere's disease. Laryngoscope 2007;117:415–20.

[5] Committee on Hearing and Equilibrium guidelines for the diagnosis and evaluation of therapy in Meniere's disease. American Academy of Otolaryngology-Head and Neck Foundation, Inc. Otolaryngol Head Neck Surg 1995;113:181–5.

[6] Alford BR. Report of subcommittee on equilibrium and its measurement. Meniere's disease: criteria for diagnosis and evaluation of therapy for reporting. Trans Am Acad Opthalmol Otolaryngol 1972;76:1462–4.

[7] Schuknecht HF, Suzuka Y, Zimmermann C. Delayed endolymphatic hydrops and its relationship to Meniere's disease. Ann Otol Rhinol Laryngol 1990;99:843–53.

[8] Kasai S, Teranishi M, Katayama N, Sugiura M, Nakata S, Sone M, et al. Endolymphatic space imaging in patients with delayed endolymphatic hydrops. Acta Otolaryngol 2009;129:1169–74.

[9] Nakashima T, Yanagita N. Outcome of sudden deafness with and without vertigo. Laryngoscope 1993;103:1145–9.

[10] Naganawa S, Sugiura M, Kawamura M, Fukatsu H, Sone M, Nakashima T. Imaging of endolymphatic and perilymphatic fluid at 3T after intratympanic administration of gadolinium-diethylene-triamine pentaacetic acid. AJNR Am J Neuroradiol 2008;29:724–6.

[11] Naganawa S, Satake H, Kawamura M, Fukatsu H, Sone M, Nakashima T. Separate visualization of endolymphatic space, perilymphatic space and bone by a single pulse sequence; 3D-inversion recovery imaging utilizing real reconstruction after intratympanic Gd-DTPA administration at 3 Tesla. Eur Radiol 2008;18:920–4.

[12] Nakashima T, Naganawa S, Pyykkö I, Gibson WP, Sone M, Nakata S, et al. Grading of endolymphatic hydrops revealed by magnetic resonance imaging. Acta Otolaryngol Suppl 2009;560:5–8.

[13] Murofushi T, Halmagyi GM, Yavor RA, Colebatch JG. Absent vestibular evoked myogenic potentials in vestibular neurolabyrinthitis. An indicator of inferior vestibular nerve involvement?. Arch Otolaryngol Head Neck Surg 1996; 122:845–8.

[14] de Waele C, Huy PT, Diard JP, Freyss G, Vidal PP. Saccular dysfunction in Meniere's disease. Am J Otol 1999;20:223–32.

[15] Ushio M, Iwasaki S, Chihara Y, Kawahara N, Morita A, Saito N, et al. Is the nerve origin of the vestibular schwannoma correlated with vestibular evoked myogenic potential, caloric test, and auditory brainstem response? Acta Otolaryngol 2009;129:1095–100.

[16] Yamamoto M, Teranishi M, Naganawa S, Otake H, Sugiura M, Iwata T, et al. Relationship between the degree of endolymphatic hydrops and electrocochleography. Audiol Neurootol 2009;15:254–60.

[17] Teranishi M, Naganawa S, Katayama N, Sugiura M, Nakata S, Sone M, et al. Image evaluation of endolymphatic space in fluctuating hearing loss without vertigo. Eur Arch Otorhinolaryngol 2009;266:1871–7.

[18] Miyagawa M, Fukuoka H, Tsukada K, Oguchi T, Takumi Y, Sugiura M, et al. Endolymphatic hydrops and therapeutic effects are visualized in 'atypical' Meniere's disease. Acta Otolaryngol 2009;129:1326–9.

[19] Sone M, Naganawa S, Teranishi M, Nakata S, Katayama N, Nakashima T. Changes in endolymphatic hydrops in a patient with Meniere's disease observed using magnetic resonance imaging. Auris Nasus Larynx 2009 Jun 18 [Epub ahead of print].

[20] Seo T, Node M, Yukimasa A, Sakagami M. Furosemide loading vestibular evoked myogenic potential for unilateral Meniere's disease. Otol Neurotol 2003;24:283–8.

Magn Reson Med Sci, Vol. 8, No. 4, pp. 187-191, 2009

CASE REPORT

Detection of Presumed Hemorrhage in the Ampullar Endolymph of the Semicircular Canal: A Case Report

Shinji NAGANAWA[1]*, Shunichi ISHIHARA[1], Shingo IWANO[1], Michihiko SONE[2], and Tsutomu NAKASHIMA[2]

Departments of [1]Radiology and [2]Otorhinolaryngology, Nagoya University Graduate School of Medicine
65 Tsurumai-cho, Shouwa-ku, Nagoya 466-8550, Japan
(Received May 1, 2009; Accepted July 8, 2009)

We examined a 61-year-old woman with sudden left-side hearing loss accompanied by severe vertigo. High signal in the ampullar endolymph of the left semicircular canal on magnetic resonance (MR) fluid attenuated inversion recovery (3D-FLAIR) images suggested labyrinthine hemorrhage. The patient had been treated for chronic heart failure and prescribed 100 mg/day of acetylsalicylic acid (aspirin) for its antiplatelet effect. The 3D-FLAIR images demonstrated a small amount of focal hemorrhage in the labyrinthine fluid that may have been overlooked on T_1-weighted images.

Keywords: ***ampulla, endolymphatic hydrops, hemorrhage, labyrinth, magnetic resonance***

Introduction

The sensitivity of 3D-FLAIR (fluid attenuated inversion recovery) to subtle alterations in the composition of labyrinthine lymph fluid in various inner ear disorders has been reported.[1-6] Combined with intratympanic Gd-DTPA administration, 3D-FLAIR has enabled separate visualization of endo- and perilymph fluid.[7] In an exceptional case of enlarged endolymphatic duct and sac syndrome, 3D-FLAIR without contrast revealed endolymphatic hydrops by visualizing the reflux of hemorrhagic fluid from the enlarged sac to the cochlea and vestibule.[8]

Although inner ear hemorrhage has been reported in many cases of sudden deafness, such as in patients with leukemia and those receiving anticoagulant therapy,[9-11] we do not believe that focal inner ear hemorrhage, such as that confined to the ampulla of the semicircular canal, has been reported.

We present the case of a patient receiving antiplatelet therapy who suffered hemorrhage confined primarily to the ampullar endolymph of the semicircular canal that was detected by 3D-FLAIR.

*Corresponding author, Phone: +81-52-744-2327, Fax: +81-52-744-2335, E-mail: naganawa@med.nagoya-u.ac.jp

Case Report

A 61-year-old woman with long-term moderate bilateral hearing loss of about 50 dB on average presented with fullness in the left ear and worsening left-side hearing loss accompanied by severe vertigo. Hearing in her left ear worsened to 80 dB on average. She had been treated for chronic heart failure and prescribed 100 mg/day of acetylsalicylic acid (aspirin) for its antiplatelet effect. Otoscopic findings were unremarkable. Bone algorithm, thin-section computed tomographic (CT) images targeting the temporal bone revealed no abnormality. The patient received oral steroid therapy but did not recover her left-ear hearing level. Two months after the onset of her profound left-ear hearing loss and severe vertigo, we obtained pre- and post-contrast MR images on a 3-tesla MR imaging scanner (Trio, Siemens Medical Solutions, Erlangen, Germany) using a 32-channel coil. For the pre-contrast scan, we performed 3D-CISS (constructive interference in the steady state), 3D-FLAIR using SPACE (sampling perfection with application-optimized contrasts by using different flip angle evolutions), and 3D T_1-weighted volume interpolated breath-hold examination with water excitation (3D-VIBE). The scan parameters of 3D-FLAIR were: repetition time, 9000 ms; echo time, 458 ms; inversion time, 2500 ms; 0.8-mm slice thickness; 0.7-mm × 0.7-mm in-plane resolution; and scan time, 5.5 min. A slice thickness of 0.8 mm was used for 3D-CISS and 3D-

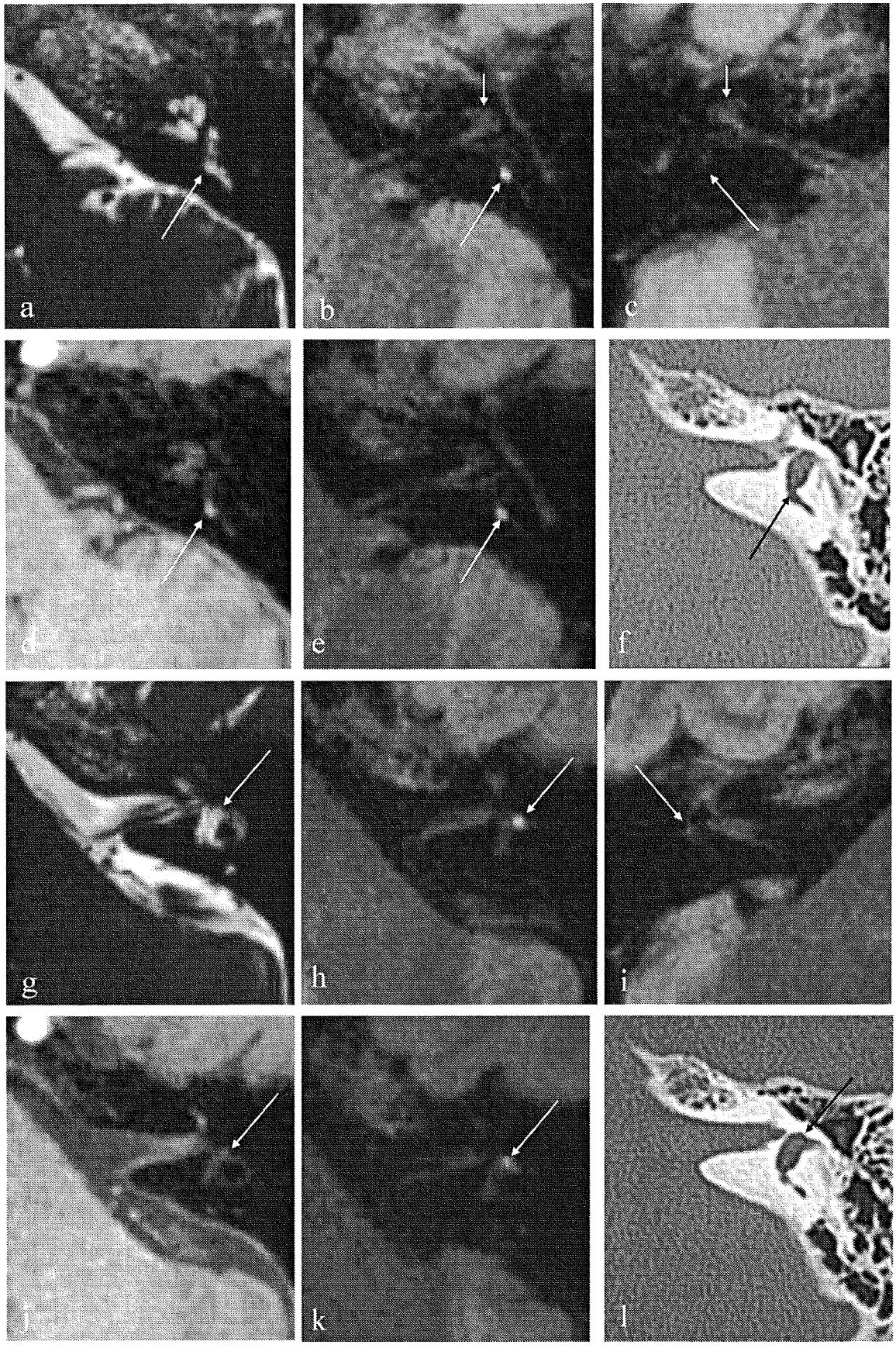

Fig. 1.

VIBE as well. Detailed parameters for 3D-CISS and 3D-VIBE were described previously.[12] Three minutes after intravenous administration of Gd-DTPA, 3D-VIBE and 3D-FLAIR were repeated.

MR images obtained with 3D-CISS showed no vestibular schwannoma and no malformation of the inner ear. High signal in the ampullar endolymph of the left lateral and posterior semicircular canal on 3D-FLAIR suggested endolymphatic hemorrhage in the subacute phase (Fig. 1). On 3D-CISS, these areas showed high signal similar to that of lymph fluid. These areas showed slightly increased signal on T_1-weighted 3D-VIBE images but were difficult to detect prospectively without first examining 3D-FLAIR images. These areas of increased signal in the ampulla corresponded with endolymphatic space in the ampulla visualized on 3D-real inversion recovery (IR) images obtained from another patient with Meniere's disease after intratympanic administration of Gd-DTPA (Fig. 2). The other areas of labyrinthine fluid, including the cochlea of the left ear, showed slightly increased signal on 3D-FLAIR. After intravenous administration of Gd-DTPA, no significant enhancement was noted. No remarkable findings were noted for the inner ear of the other side.

Discussion

The endolymphatic space of the ampulla in the semicircular canal contains the crista ampullaris, where rich vascular structure has been observed on histological sections.[13-15] In animals, hemorrhage has been reported to cause temporary and permanent inner ear damage.[16] Hemorrhage in the ampullar endolymph would cause deterioration of the crista ampullaris resulting in severe vertigo.

It is not clear why our patient's hemorrhage was limited mostly to the ampullar endolymph. The cupula on the crista ampullaris may be vulnerable to mechanical stress,[17] but hemorrhage in the ampulla of the semicircular canal is rare and not reported.

Our patient underwent MR imaging 2 months after the onset of symptoms. If the symptoms were caused by hemorrhage from vascular structures in the crista ampullaris, it is unclear why hemorrhage remained there for about 2 months. Small amounts of continuous bleeding may have been present, although such hemorrhage would likely be visible even on 3D-VIBE, and Gd-DTPA might enhance signal on post-contrast 3D-FLAIR.

In the present case, hemorrhage was not dense enough to be detected on T_1-weighted 3D-VIBE images. We speculate that the methohemoglobin concentration of this subacute hemorrhage was too low to be detected on 3D-VIBE. The possibility remains that a T_1-shortening pathology other than methohemoglobin, such as increased protein concentration, may have been present. However, our patient's middle ear and mastoid air cells were clear,

Fig. 1. A 61-year-old woman with long-term moderate bilateral hearing loss presented with left ear fullness and additional left-side hearing loss accompanied by severe vertigo (**a-f**; slices at the posterior ampulla level, **g-l**; slices at the lateral ampulla level).

a) 3D-CISS (constructive interference in the steady state) image of the left ear shows that the ampulla of the posterior semicircular canal (arrow) is filled with high signal similar to cerebrospinal fluid.

b) 3D-FLAIR (fluid attenuated inversion recovery) image of the left ear shows remarkably high signal in the posterior ampulla (arrow) and slightly increased signal in the cochlea (short arrow).

c) 3D-FLAIR image of the right ear shows no signal increase in the posterior ampulla (arrow) and cochlea (short arrow).

d) 3D T_1-weighted VIBE (volume interpolated breath-hold examination with water excitation) image of the left ear shows slightly elevated signal in the posterior ampulla (arrow), but this might be difficult to notice without 3D-FLAIR.

e) Post-contrast 3D-FLAIR image of the left ear shows no signal enhancement by Gd-DTPA in the posterior ampulla (arrow) compared to pre-contrast 3D-FLAIR (**b**).

f) Computed tomographic (CT) image of the left ear shows no abnormal finding around the posterior ampulla (arrow).

g) 3D-CISS image of the left ear shows that the ampulla of the lateral semicircular canal (arrow) is filled with high signal similar to that of cerebrospinal fluid.

h) 3D-FLAIR image of the left ear shows remarkably high signal in the lateral ampulla (arrow).

i) 3D-FLAIR image of the right ear shows no signal increase in the lateral ampulla (arrow).

j) 3D T_1-weighted VIBE image of the left ear shows slightly elevated signal in the lateral ampulla (arrow); however, this high signal might be difficult to notice without 3D-FLAIR.

k) Post-contrast 3D-FLAIR image of the left ear shows no signal enhancement with Gd-DTPA in the lateral ampulla (arrow) compared to pre-contrast 3D-FLAIR (**b**).

l) CT image of the left ear shows no abnormal finding around the lateral ampulla (arrow).

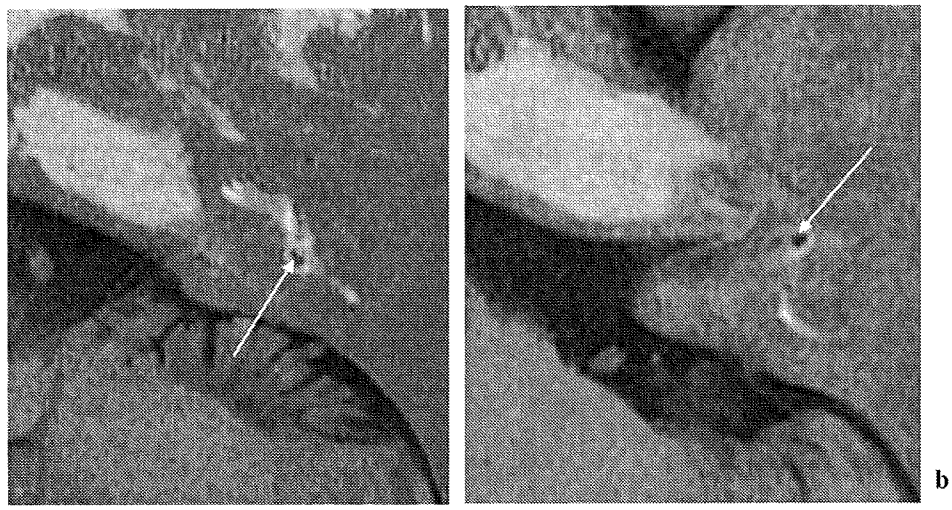

Fig. 2. Reference images from a different patient with Meniere's disease. This 3D real-inversion recovery (IR) image was obtained after intratympanic injection of Gd-DTPA.
a) A negative signal area indicating endolymph space in the posterior ampulla (arrow) seems to correspond to the area of high signal on 3D-FLAIR (fluid attenuated inversion recovery) (Fig. 1**b**) in the present case.
b) A negative signal area indicating endolymph space in the lateral ampulla (arrow) seems to correspond to the area of high signal on 3D-FLAIR (Fig. 1**h**) in the present case.

and there was no sign of meningitis. Thus, we believe that methohemoglobin caused the high ampullar signal on 3D-FLAIR.

Labyrinthine hemorrhage has been attributed to coagulopathy, tumor, trauma, viral labyrinthitis, serofibrinoid labyrinthitis after stapes surgery, cholesterol granuloma, lupus erythematosus, and other causes.[5,18]

3D-FLAIR is more sensitive than T_1-weighted imaging in detecting subtle compositional changes of lymph fluid.[4] In the present case, focal hemorrhage of the inner ear, which might have been overlooked on T_1-weighted images, could be detected by adding 3D-FLAIR. Precontrast T_1-weighted imaging has been included in the MR imaging protocol for inner ear diseases to detect inner ear hemorrhage[18] such as that in the present case, but the more sensitive 3D-FLAIR sequence should be included to detect subtle pathologies.

To our knowledge, hemorrhage limited to the ampullar endolymph has not been reported. It might be speculated that it has long been overlooked by MR imaging without 3D-FLAIR images.

In patients with acute vertigo undergoing anticoagulant therapy, 3D-FLAIR may impact clinical management, although further accumulation of such cases is necessary before general conclusions can be drawn. Thus, radiologists should at least be aware of this finding.

References

1. Otake H, Sugiura M, Naganawa S, Nakashima T. 3D-FLAIR magnetic resonance imaging in the evaluation of mumps deafness. Int J Pediatr Otorhinolaryngol 2006; 70:2115–2117.
2. Sugiura M, Naganawa S, Nakata S, Kojima S, Nakashima T. 3D-FLAIR MRI findings in a patient with Ramsay Hunt syndrome. Acta Otolaryngol 2007; 127:547–549.
3. Sugiura M, Naganawa S, Sato E, Nakashima T. Visualization of a high protein concentration in the cochlea of a patient with a large endolymphatic duct and sac, using three-dimensional fluid-attenuated inversion recovery magnetic resonance imaging. J Laryngol Otol 2006; 120:1084–1086.
4. Sugiura M, Naganawa S, Teranishi M, Nakashima T. Three-dimensional fluid-attenuated inversion recovery magnetic resonance imaging findings in patients with sudden sensorineural hearing loss. Laryngoscope 2006; 116:1451–1454.
5. Sugiura M, Naganawa S, Teranishi M, Sato E, Kojima S, Nakashima T. Inner ear hemorrhage in systemic lupus erythematosus. Laryngoscope 2006; 116:826–828.
6. Yoshida T, Sugiura M, Naganawa S, Teranishi M, Nakata S, Nakashima T. Three-dimensional fluid-attenuated inversion recovery magnetic resonance imaging findings and prognosis in sudden sensorineural hearing loss. Laryngoscope 2008; 118: 1433–1437.

7. Nakashima T, Naganawa S, Sugiura M, et al. Visualization of endolymphatic hydrops in patients with Meniere's disease. Laryngoscope 2007; 117: 415-420.
8. Naganawa S, Sone M, Otake H, Nakashima T. Endolymphatic hydrops of the labyrinth visualized on noncontrast MR imaging: a case report. Magn Reson Med Sci 2009; 8:43-46.
9. Sando I, Egami T. Inner ear hemorrhage and endolymphatic hydrops in a leukemic patient with sudden hearing loss. Ann Otol Rhinol Laryngol 1977; 86:518-524.
10. Vellin JF, Bozorg Grayeli A, Cyna-Gorse F, Refass A, Bouccara D, Sterkers O. [Labyrinthine hemorrhage caused by anticoagulant therapy]. Ann Otolaryngol Chir Cervicofac 2005; 122:194-197. [Article in French]
11. Shinohara S, Yamamoto E, Saiwai S, et al. Clinical features of sudden hearing loss associated with a high signal in the labyrinth on unenhanced T_1-weighted magnetic resonance imaging. Eur Arch Otorhinolaryngol 2000; 257:480-484.
12. Naganawa S, Satake H, Iwano S, Fukatsu H, Sone M, Nakashima T. Imaging endolymphatic hydrops at 3 tesla using 3D-FLAIR with intratympanic Gd-DTPA administration. Magn Reson Med Sci 2008; 7:85-91.
13. Lyon MJ, Wanamaker HH. Blood flow and assessment of capillaries in the aging rat posterior canal crista. Hear Res 1993; 67:157-165.
14. Mazzoni A. The vascular anatomy of the vestibular labyrinth in man. Acta Otolaryngol Suppl 1990; 472:1-83.
15. Nomura Y, Hiraide F. The capillary in the human vestibular labyrinth. A histochemical staining technique. Ann Otol Rhinol Laryngol 1969; 78:1220-1226.
16. Radeloff A, Unkelbach MH, Tillein J, et al. Impact of intrascalar blood on hearing. Laryngoscope 2007; 117:58-62.
17. Nomura Y. Vestibule, In: Morphology in otology. Tokyo: Chugai-igaku-sha, 2006; 101-115.
18. Swartz J, Harnsberger H. The otic capsule and otodystrophies, In: Imaging of the temporal bone third edition. New York: Thieme, 1998; 284-285.

Technical Note

Three-Dimensional (3D) Visualization of Endolymphatic Hydrops after Intratympanic Injection of Gd-DTPA: Optimization of a 3D-Real Inversion-Recovery Turbo Spin-Echo (TSE) Sequence and Application of a 32-Channel Head Coil at 3T

Shinji Naganawa, MD,[1]* Shunichi Ishihara, MD,[1] Shingo Iwano, MD,[1] Michihiko Sone, MD,[2] and Tsutomu Nakashima, MD[2]

Purpose: To enable volume visualization of endolymphatic hydrops of Ménière's disease via a volume rendering (VR) technique, a three-dimensional (3D) inversion-recovery (IR) sequence with real reconstruction (3D-real IR) sequence after intratympanic injection of Gd-DTPA was optimized for higher spatial resolution using a 32-channel head coil at 3T.

Materials and Methods: Pulse sequence parameters were optimized using a diluted Gd-DTPA phantom. Then, 11 patients who had been clinically diagnosed with Ménière's disease and a patient with sudden hearing loss were scanned. Images were processed using commercially available 3D-VR software. 3D-real IR data was processed to produce endolymph and perilymph fluid volume images in different colors. 3D-CISS data was processed to generate total fluid volume images.

Results: While maintaining a comparable signal-to-noise ratio (SNR) and scan time, the voxel volume could be reduced from 0.4 × 0.4 × 2 mm^3 with a 12-channel coil to 0.4 × 0.4 × 0.8 mm^3 with a 32-channel coil. A newly-optimized protocol allowed the smooth, three-dimensional visualization of endolymphatic hydrops in all patients with Ménière's disease.

Conclusion: Volumetrically separate visualization of endo-/perilymphatic space is now feasible in patients with Ménière's disease using an optimized 3D-real IR sequence, a 32-channel head coil, at 3T, after intratympanic administration of Gd-DTPA. This will aid the understanding of the pathophysiology of Ménière's disease.

Key Words: magnetic resonance imaging; 3D imaging; ADVANCED imaging techniques; temporal bone disease; labyrinth

J. Magn. Reson. Imaging 2010;31:210–214.

MÉNIÈRE's DISEASE is not a rare disease. Its prevalence has been reported to be 43 per 100,000 and an average annual incidence has been reported to be 4.3 per 100,000 (1). For a conclusive diagnosis of Ménière's disease, histopathologic confirmation is necessary; however, it is virtually impossible to obtain such histological confirmation in patients. An imaging method capable of visualizing endolymphatic hydrops has long been desired.

Recently, separate visualization of endo- and perilymphatic space was made possible for the first time in living human patients by the intratympanic injection of Gd-DTPA and three-dimensional (3D)–fluid-attenuated inversion-recovery (FLAIR) at 3T (2).

Soon after that, separate images visualizing endolymphatic space and perilymphatic space could be obtained using two different inversion times to null either Gd-containing perilymph or non-Gd-containing endolymph (3). Fusion of the two images allowed simultaneous appreciation of the spatial relationships between endo- and perilymphatic space (3).

Finally, a 3D–inversion-recovery (IR) sequence with real reconstruction (3D-real IR) at 3T made it possible to separately visualize endolymph, perilymph and bone using a single pulse sequence (4). These three techniques were applied at 3T using a 12-channel head coil.

Labyrinthine structure is very complex; thus, 3D visualization of endo-/perilymph space is desirable

[1]Department of Radiology, Nagoya University Graduate School of Medicine, Nagoya, Japan.

[2]Department of Otorhinolaryngology, Nagoya University Graduate School of Medicine, Nagoya, Japan.

*Address reprint requests to: S.N., Department of Radiology, Nagoya University Graduate School of Medicine, 65 Tsurumai-cho, Shouwa-ku, Nagoya 466-8550, Japan. E-mail: naganawa@med.nagoya-u.ac.jp

Received April 15, 2009; Accepted October 5, 2009.

DOI 10.1002/jmri.22012

Published online in Wiley InterScience (www.interscience.wiley.com).

for the proper diagnosis and understanding of the pathophysiology of Ménière's disease (5). However, due to the low signal-to-noise ratio (SNR) of the above-mentioned three methods, a slice thickness as thick as 2 mm was necessary, even with a 15-minute scan time at 3T for one volume acquisition.

Faster scan using 3D-FLAIR provided by the "sampling perfection with application optimized contrast using different flip angle evolutions" (SPACE) sequence has been tried with a slice thickness of 0.8 mm; however, visualization of cochlear endolymphatic hydrops was not satisfactory due to image blurring (6).

The purpose of this study was to increase the spatial resolution through further optimization of the sequence and by employing a 32-channel head coil (7), and thereby take on the challenge of visualizing endolymphatic hydrops in 3D.

MATERIALS AND METHODS

All scans were performed on a 3T MR scanner (MAGNETOM Trio-TIM; Siemens Medical Solutions, Erlangen, Germany) using commercially available 12-channel and 32-channel array head coils from the same vendor as the scanner.

First, the SNR of a polyvinyl alcohol gel (PVA) phantom was compared between the 12-channel and 32-channel head coils.

Then, using a diluted Gd-DTPA phantom, a 3D-real IR sequence was optimized to obtain a higher spatial resolution than previously reported protocol (4). We assumed that the scan time should be kept within 15 minutes, which is nearly the limit for patients. Based on an earlier pilot study, we assumed that the concentration of Gd-DTPA in the labyrinth after intratympanic injection was approximately 1/16,000 that of the original solution. Repetition time (TR), echo time (TE), inversion time (TI), and echo train length (ETL) of the turbo-spin-echo (TSE) readout were optimized to fulfill the following conditions: a scan time of 15 minutes; higher time efficiency in terms of contrast-to-noise ratio (CNR); and higher spatial resolution than the previously reported protocol (4). The contrast between saline and 1/16,000-diluted Gd solution was used to compute the CNR for the optimization. The range of TR values that was measured and evaluated was 2000–12,000 msec, and that of TE was 122–328 msec. Various combinations of TI and ETL were tried, with TI in the range of 1100–1700 msec and ETL in the range of 15–43 msec. The previously reported protocol employed the following values: TR = 9000 msec, TE = 134 msec, TI = 1700 msec, and ETL = 23 (4).

Twelve patients, 11 with a clinical diagnosis of Ménière's disease and one with sudden sensorineural hearing loss, received an intratympanic injection of eight-fold-diluted Gd-DTPA according to the previously reported procedure (2). Twenty-four hours after the injection, they were scanned using the newly-optimized method and a 32-channel coil. This study was approved by the medical ethics committee of the hospital, and informed consent was obtained from all patients.

As an anatomical reference, MR cisternography was measured with the 3D–constructive interference in the steady state (CISS) technique in each patient, with 0.4-mm isotropic voxels, TR = 6.4 msec, TE = 3.2 msec, and flip angle = 50 degrees.

The diagnosis of endolymphatic hydrops using 3D-real IR images was made based on the previously reported grading criteria (8).

3D–volume rendering (VR) was performed using commercially available 3D-VR software (INTAGE Realia professional, KGT LTD, Tokyo, Japan) that runs on a Windows PC. DICOM data was transferred offline to the PC.

3D-real IR images were manipulated on the PC by an experienced neuroradiologist. First, the labyrinthine area was contoured manually; then endolymphatic fluid and perilymphatic fluid were segmented by signal intensity thresholding. Generally, endolymphatic-space voxels have negative signal values; the surrounding bone voxels have near-zero signal, and perilymph space voxels have positive signal values.

Subtle adjustments were performed subjectively by slightly changing the thresholds and the slope/shape of the opacity curve while observing the 3D-VR images. When deciding these parameters, a VR image revealing the whole of labyrinthine lymph fluid space, computed from 3D-CISS images, was taken into account in terms of the shape and size (morphological proportion) of the labyrinth.

RESULTS

In a PVA phantom measurement, the 32-channel coil showed a 25% higher SNR than that of the 12-channel coil at a distance of 3.5 cm from the center (the vicinity of the inner ear).

CNR per unit time was optimized. The optimized protocol showed a 40% higher CNR per unit time than that of the previously reported protocol (4). Hence, the voxel volume of the newly-optimized protocol for the 32-channel head coil was decreased by 60% from the previous 0.4 × 0.4 × 2.0 mm^3 to 0.4 × 0.4 × 0.8 mm^3.

Details of the newly-optimized 3D-real IR protocol using the 32-channel head coil were as follows: sequence type, conventional 3D TSE with constant flip angles of 180 degrees for the TSE train, TR = 6000 msec, TE = 182 msec, TI = 1500 msec, inversion pulse, slab selective, ETL = 27, echo spacing = 12.2 msec, FOV = 160 mm, matrix size = 384 × 384 × 30, slices thickness = 0.8 mm with a slice partial-Fourier factor = 6/8, bandwidth = 213 Hz/pixel, and reconstruction mode = "real." A parallel imaging technique (generalized autocalibrating partially parallel acquisitions [GRAPPA]) was employed with an acceleration factor of 2, and the scan time was 15 minutes.

Optimized 3D-real IR images provided anatomically appropriate visualization of enlarged endolymphatic space as negative signal, perilymph space containing

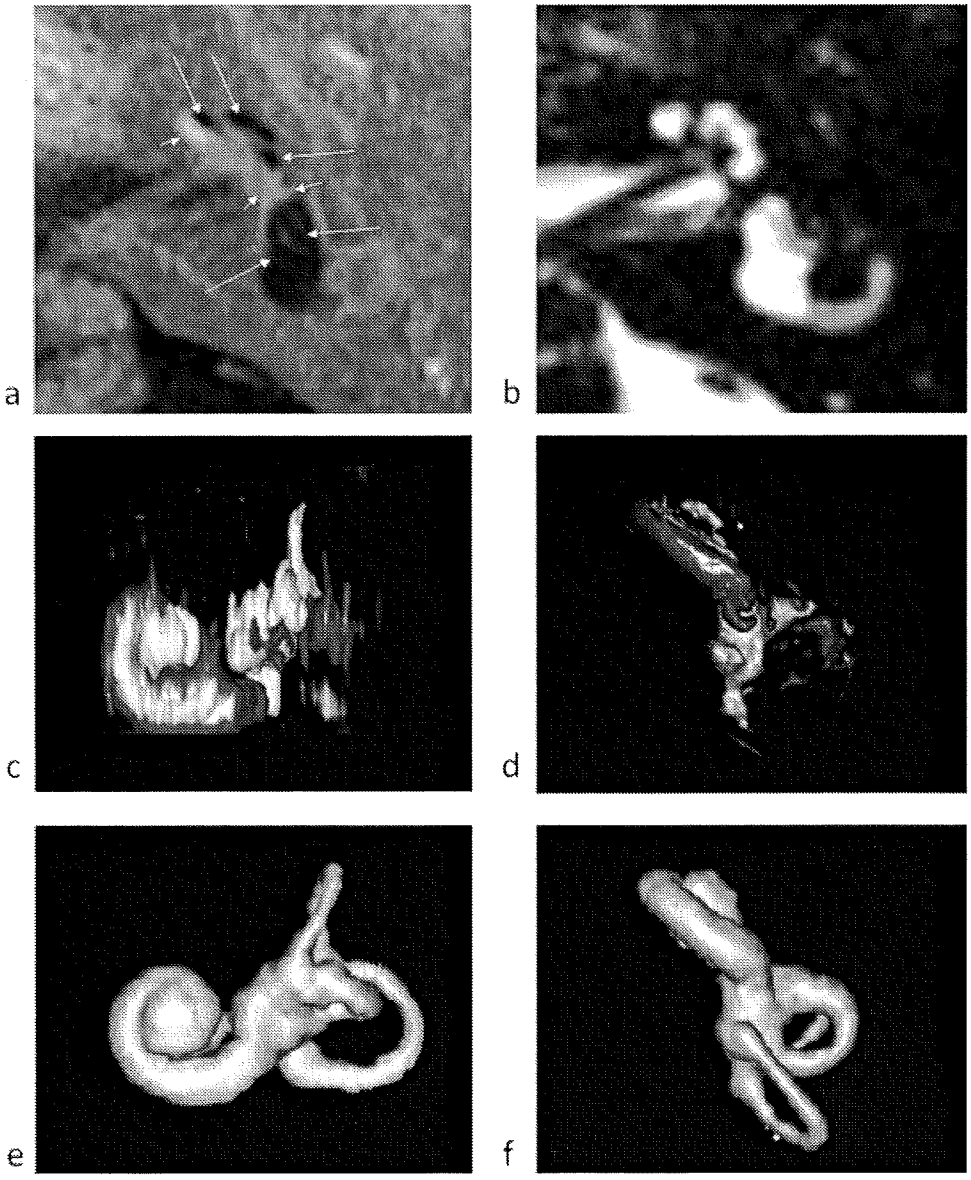

Figure 1. A 65-year-old man with left-side Ménière's disease. **a**: This 3D-real IR image shows enlarged endolymphatic space (arrows) as negative signal and perilymph space as positive signal (short arrows). The severely enlarged cochlear duct (endolymphatic space in the cochlea) is far larger than the scala vestibuli. Almost all of the vestibular space is occupied by endolymph. **b**: On this 3D-CISS image, high signal in the labyrinth reveals total fluid space. **c,d**: 3D volume-rendered (VR) images of 3D-real IR. Lateral view (c) and superior-facing (foot-to-head) view (d). These show volumetric views of perilymph/endolymph space in different colors. Perilymph space is shown in blue, and endolymph space is shown in yellow. **e,f**: 3D-VR image of CISS. Lateral view (e) and superior-facing view (f). These reveal total fluid space.

diffused Gd as high signal, and surrounding bone as zero signal in all patients (Fig. 1a). 3D-CISS images revealed the entire fluid space (Fig. 1b). In all patients, the optimized 3D-real IR sequence enabled 3D visualization of perilymph space and endolymph space in different colors by VR. The degree and spatial distribution of endolymphatic hydrops can be well appreciated (Fig. 1c and d) by comparing with the 3D-VR of total fluid space (endolymph + perilymph) based on 3D-CISS (Fig. 1e and f).

Using this commercially available software, VR images of perilymph space alone can also be generated (Fig. 2a). The spatial relationship between endolymph and perilymph can be well appreciated by comparing the perilymph-only image to the combined, color-coded perilymph+endolymph image (Fig. 2b). In a patients with sudden sensorineural hearing loss, no endolymphatic hydrops was observed (Fig. 3).

DISCUSSION

Volumetric presentation of the labyrinthine fluid space has been reported previously for the entire fluid space based on 3D-fast spin echo data (9), and on 3D-CISS data (10). Virtual endoscopic presentations without the separation of endo-/perilymph space have also been reported (11).

Using data from a histological specimen, a 3D presentation of endolymphatic hydrops has recently been reported based on manual segmentation of endo-/perilymph space on each section (5).

Even with the optimization using a 32-channel coil at 3T, 3D-VR images computed from source images with a 0.4 × 0.4 × 0.8 mm^3 resolution (the present study) are still coarse compared to those based on 10-μm-thick histological sections (5). However, this is the first report of 3D visualization of endolymphatic hydrops in living human subjects.

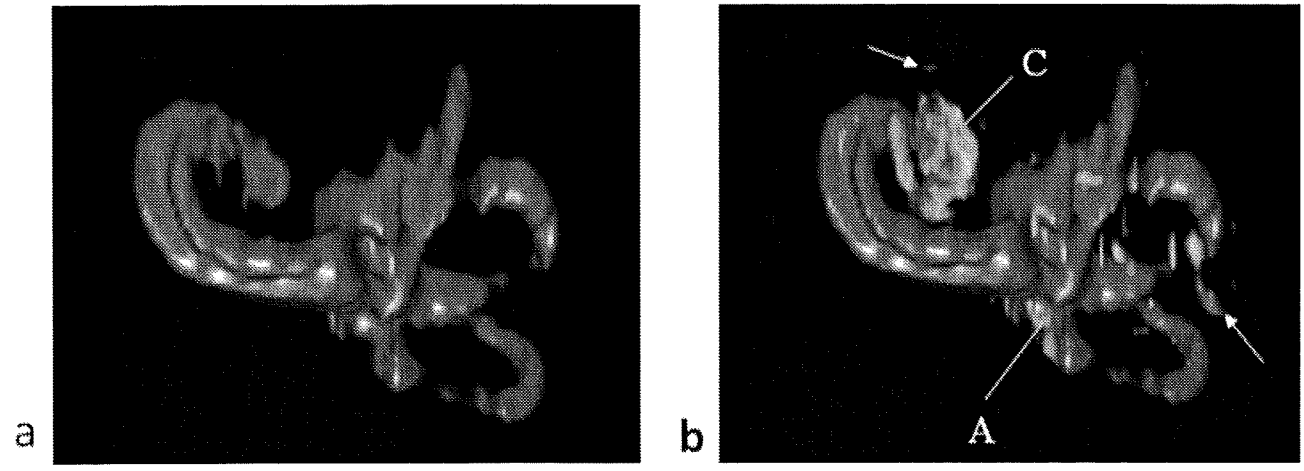

Figure 2. A 57-year-old man with left-side Ménière's disease. **a**: 3D–volume-rendering (VR) of only perilymph space. Perilymph space is shown in blue. **b**: 3D-VR of perilymph/endolymph space in different colors. Endolymph space in the cochlear turns (C), and ampulla (A) are shown in yellow. Structures caused by noise are also apparent (arrows). In this patient, endolymphatic hydrops in the cochlea and vestibule are not so severe as the previous case shown on Fig. 1.

When the distribution of Gd-DTPA into some parts of the labyrinth is fainter, the segmentation of those parts might be difficult. This is especially true in the apical turn of the cochlea, where the enhancement of perilymph tends to be fainter than the basal turn in most patients. And in case of severe endolymphatic hydrops of the vestibule, the concentration of Gd-DTPA in the semicircular canals tends to be relatively low as a result of blockage due to enlarged vestibular endolymph as seen on Fig. 1.

The 32-channel head coil provided higher SNRs compared to the 12-channel coil; however, signal uniformity within the field of view was inferior to that of the 12-channel coil. Decreased uniformity of signal intensity might adversely affect the intensity thresholding used for volume segmentation. However, the present method using 3D-real IR separates the perilymph signal and endolymph signal into positive and negative polarities so that the segmentation does not depend only on differences in positive signal intensity. Thus, the lower signal uniformity of the 32-channel coil can be compensated to some degree by using the real reconstruction technique.

Even with 3D-real IR, however, the segmentation is somewhat vulnerable to subjective bias because the thresholds are adjusted manually. Furthermore, a small threshold change alters the size of each space significantly. These two points should be improved for

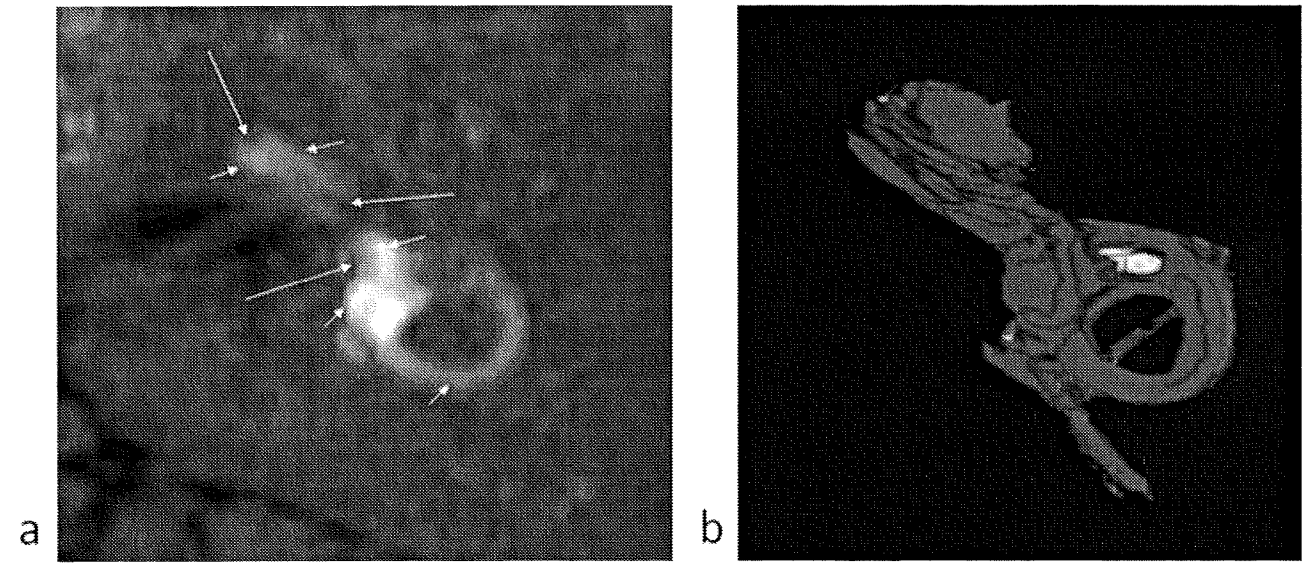

Figure 3. A 54-year-old woman with left-side sudden sensorineural hearing loss. **a**: This 3D-real inversion-recovery (IR) image shows nondilated endolymphatic space (arrows) as negative signal and perilymph space as positive signal (short arrows). **b**: 3D volume-rendered (VR) images of 3D-real IR. Superior-facing (foot-to-head) view. The volumetric view of perilymph/endolymph space is shown in different colors. Perilymph space is shown in blue, and endolymph space is shown in yellow. Note that the endolymphatic space is much smaller in this patient without endolymphatic hydrops compared to that in the patient with endolymphatic hydrops (Fig. 1d).

more reliable volume quantification of lymph fluid in the future. From the histological specimen, endolymphatic volume has been quantified. In control subjects, the average volume ratio of endolymphatic space in total lymph fluid was 20% from the histological data (12). In the patient shown on Fig. 1, it was calculated as 50% by 3D-VR software.

A rupture of Reissner's membrane would complicate the separation of endo-/perilymph based on differences in Gd-DTPA concentration due to the contamination of each space. However, in temporal bone autopsies of bilateral Ménière's disease, only 2.8% of cases showed endolymphatic collapse, suggesting the rupture. In the present study, Reissner's membrane did not rupture in any patient of the present study. In a previously reported case, non-contrast-enhanced MR images revealed a reflux of proteinous or hemorrhagic fluid into enlarged endolymphatic space in the labyrinth in a patient with enlarged endolymphatic duct and sac syndrome (13). In this particular patient, there was a rupture in one ear after head trauma. In animal experiments, the rupture occurs mostly in the acute and excessive hydrops (14). Therefore, the rupture might occur in some condition; however, it is not so frequent in the patients with Ménière's disease.

3D-VR of perilymph space can be generated from 3D-FLAIR images, and total lymphatic space can be imaged by 3D-CISS. Subtraction of the perilymph space from total lymphatic space should reveal endolymphatic space. However, the subtraction of such small, separately-acquired volumes might be degraded by substantial spatial misregistration. Segmentation based on a single imaging sequence such as 3D-real IR, as shown in the present study, would be more reliable.

In conclusion, the optimized method described here, combined with a 32-channel coil at 3T, might open the door to the 3D visualization of each of the lymphatic spaces for the precise understanding of Ménière's disease.

REFERENCES

1. Kotimaki J, Sorri M, Aantaa E, Nuutinen J. Prevalence of Meniere disease in Finland. Laryngoscope 1999;109:748–753.
2. Nakashima T, Naganawa S, Sugiura M, et al. Visualization of endolymphatic hydrops in patients with Meniere's disease. Laryngoscope 2007;117:415–420.
3. Naganawa S, Sugiura M, Kawamura M, Fukatsu H, Sone M, Nakashima T. Imaging of endolymphatic and perilymphatic fluid at 3T after intratympanic administration of gadolinium-diethylene-triamine pentaacetic acid. AJNR Am J Neuroradiol 2008;29:724–726.
4. Naganawa S, Satake H, Kawamura M, Fukatsu H, Sone M, Nakashima T. Separate visualization of endolymphatic space, perilymphatic space and bone by a single pulse sequence; 3D-inversion recovery imaging utilizing real reconstruction after intratympanic Gd-DTPA administration at 3 Tesla. Eur Radiol 2008;18:920–924.
5. Teranishi M, Yoshida T, Katayama N, et al. 3D computerized model of endolymphatic hydrops from specimens of temporal bone. Acta Otolaryngol 2009;129:43–47.
6. Naganawa S, Satake H, Iwano S, Fukatsu H, Sone M, Nakashima T. Imaging endolymphatic hydrops at 3 Tesla using 3D-FLAIR with intratympanic Gd-DTPA administration. Magn Reson Med Sci 2008;7:85–91.
7. Wiggins GC, Triantafyllou C, Potthast A, Reykowski A, Nittka M, Wald LL. 32-channel 3 Tesla receive-only phased-array head coil with soccer-ball element geometry. Magn Reson Med 2006;56:216–223.
8. Nakashima T, Naganawa S, Pyykko I, et al. Grading of endolymphatic hydrops using magnetic resonance imaging. Acta Otolaryngol 2009;129:5–8.
9. Neri E, Caramella D, Cosottini M, et al. High-resolution magnetic resonance and volume rendering of the labyrinth. Eur Radiol 2000;10:114–118.
10. Kim HJ, Song JW, Chon KM, Goh EK. Common crus aplasia: diagnosis by 3D volume rendering imaging using 3DFT-CISS sequence. Clin Radiol 2004;59:830–834.
11. Naganawa S, Iwayama E, Koshikawa T, et al. Virtual endoscopy of the labyrinth, using a 3D-FastASE sequence. J Magn Reson Imaging 2001;13:792–796.
12. Teranishi M, Yoshida T, Katayama N, et al. 3D computerized model of endolymphatic hydrops from specimens of temporal bone. Acta Otolaryngol Suppl 2009:43–47.
13. Naganawa S, Sone M, Otake H, Nakashima T. Endolymphatic hydrops of the labyrinth visualized on noncontrast MR imaging: a case report. Magn Reson Med Sci 2009;8:43–46.
14. Valk WL, Wit HP, Albers FW. Rupture of Reissner's membrane during acute endolymphatic hydrops in the guinea pig: a model for Meniere's disease? Acta Otolaryngol 2006;126:1030–1035.

Acta Oto-Laryngologica, 2009; Early Online, 000–000

informa
healthcare

ORIGINAL ARTICLE

3 Tesla magnetic resonance imaging obtained 4 hours after intravenous gadolinium injection in patients with sudden deafness

MITSUHIKO TAGAYA[1], MASAAKI TERANISHI[1], SHINJI NAGANAWA[2], TOMOYUKI IWATA[1], TADAO YOSHIDA[1], HIRONAO OTAKE[1], SEIICHI NAKATA[1], MICHIHIKO SONE[1] & TSUTOMU NAKASHIMA[1]

[1]*Department of Otorhinolaryngology and* [2]*Department of Radiology, Nagoya University, Graduate School of Medicine, Nagoya, Japan*

Abstract

Conclusion: 3 Tesla (3T) magnetic resonance imaging (MRI) performed 4 h after intravenous gadolinium (Gd) injection provides sufficient anatomic resolution of the inner ear fluid spaces in sudden deafness. The signal intensity ratio (SIR) between the cochlea and cerebellum may be a good indicator of disruption of the blood–labyrinthine barrier. *Objectives:* We evaluated the inner ear 4 h after intravenous Gd injection to determine whether 3T MRI enables the acquisition of images of the affected inner ear in sudden deafness. *Methods:* Ten patients underwent 3T MRI scanning 4 h after intravenous Gd injection. Three-dimensional fluid-attenuated inversion recovery (3D-FLAIR) MRI was performed. *Results:* The SIR varied from 0.45 to 2.17 in 11 affected ears and from 0.43 to 1.48 in 9 unaffected ears. The difference of contrast (affected ear vs unaffected ear) could be detected in five of the nine patients with unilateral sudden deafness. The Gd distribution was recognized in the vestibule of 10 affected ears and in the cochlea of 5 affected ears, in which no significant hydrops was observed. In the remaining vestibules and cochleas of affected ears, the Gd enhancement was too faint to evaluate the endolymphatic hydrops.

Keywords: *Inner ear fluid spaces, blood–labyrinthine barrier, gadolinium distribution, fluid-attenuated inversion recovery, endolymph, perilymph, signal intensity ratio*

Introduction

Three-dimensional fluid-attenuated inversion recovery (3D-FLAIR) magnetic resonance imaging (MRI) has been developed to detect high concentrations of protein or hemorrhage. Our previous study using a 3 Tesla (3T) MRI unit showed that 31 of 48 patients with sudden deafness had high signals in the affected inner ear before intravenous gadolinium (Gd) injection [1]. Immediately after intravenous Gd injection, 16 of the 31 ears showed Gd enhancement that suggested disruption of the blood–labyrinthine barrier. Gd enhancement of the inner ear was most intense 4 h after intravenous Gd injection [2,3]. In the present study, we evaluated the signal intensity of the inner ear 4 h after intravenous Gd injection and compared the intensity with that of the cerebellar hemisphere in patients with sudden deafness.

In patients with Ménière's disease, 1 day after the intratympanic Gd injection, 3T 3D-FLAIR MRI shows Gd enhancement in the perilymph and visualize the enlarged endolymphatic space [4]. This method requires intratympanic Gd injection. However, Gd is generally administered intravenously for contrast enhancement in MRI. In the present study, we also evaluated whether images obtained by 3T MRI 4 h after intravenous Gd injection provide sufficient anatomic resolution to image the inner ear fluid spaces in patients with sudden deafness.

Correspondence: Mitsuhiko Tagaya MD, Departmenet of Otorhinolaryngology, Nagoya University, Graduate School of Medicine, 65 Tsurumai, Showa, Nagoya, 466-8550, Japan. Fax: +81 52 744 2325. E-mail: mi-man@ra2.so-net.ne.jp

(Received 26 August 2009; accepted 28 September 2009)

ISSN 0001-6489 print/ISSN 1651-2251 online
DOI: 10.3109/00016480903384176